Fucoxanthin alleviates chondrocyte inflammation and osteoarthritis by modulating the JAK2/STAT3 signaling pathway

MIRADJ SIDDICK ADAM*, HUANGMING ZHUANG*, XUNSHAN REN*, YUELONG ZHANG and PANGHU ZHOU

Department of Orthopedics, Renmin Hospital of Wuhan University, Wuhan, Hubei 430060, P.R. China

Received February 13, 2026; Accepted April 29, 2026

DOI: 10.3892/mmr.2026.13933

Abstract. Osteoarthritis (OA) is the most common type of joint degeneration and is a leading cause of chronic disability worldwide. OA is characterized by progressive cartilage degradation, synovial inflammation and oxidative stress within the joint microenvironment. Current pharmacological treatments primarily provide symptomatic relief and are often associated with substantial adverse effects, highlighting the need for new and safe disease-modifying agents. Fucoxanthin (FUC), a carotenoid pigment found in brown algae, exhibits antioxidant, anti-inflammatory and chondroprotective properties. Although FUC may have therapeutic effects in OA, the exact mechanisms remain unclear. In the present study, in a post-traumatic OA rat model induced by anterior cruciate ligament transection, intra-articular administration of FUC (200 mg/kg) substantially protected the articular cartilage architecture and inhibited proteoglycan loss. In IL-1β-stimulated primary rat chondrocytes, FUC markedly decreased the levels of proinflammatory cytokines (IL-6 at both the mRNA and protein levels and IL-1β at the protein level) as well as cartilage-degrading enzymes (MMP3, MMP13 and a disintegrin and metalloproteinase with thrombospondin motifs 5) at the mRNA and protein levels. Furthermore, the chondroprotective and anti-inflammatory effects of FUC were largely abrogated by RO8191, a selective Janus kinase (JAK)2/STAT3 pathway activator, suggesting that inhibition of the JAK2/STAT3 signaling pathway contributes to FUC-mediated protective effects. The antioxidant capacity of FUC was evaluated using DPPH and hydroxyl radical scavenging assays, while intracellular reactive oxygen species (ROS) levels in IL-1β-stimulated chondrocytes were measured by fluorescence microscopy. FUC demonstrated a dose-dependent free radical scavenging activity and significantly reduced IL-1β-induced intracellular ROS generation in chondrocytes ($P<0.05$). These findings suggest that FUC may represent a candidate multitarget natural compound for OA that can target oxidative stress, inflammation and extracellular matrix degradation via the JAK2/STAT3 signaling axis. Future investigations should determine the optimal pharmaceutical delivery system, the pharmacokinetics and tissue distribution associated with both local and systemic delivery of FUC, as well as the long-term safety and efficacy in larger preclinical models and human trials.

Correspondence to: Professor Panghu Zhou, Department of Orthopedics, Renmin Hospital of Wuhan University, 238 Jiefang Road, Wuchang, Wuhan, Hubei 430060, P.R. China
E-mail: zhoupanghu@whu.edu.cn

*Contributed equally

Abbreviations: OA, osteoarthritis; JAK, Janus kinase; FUC, fucoxanthin; SD, Sprague-Dawley; ACLT, anterior cruciate ligament transection; ROS, reactive oxygen species; DPPH, 2,2-diphenyl-1-picrylhydrazyl; ADAMTS, a disintegrin and metalloproteinase with thrombospondin motifs; COX-2, cyclooxygenase-2; iNOS, inducible nitric oxide synthase

Key words: anti-inflammatory, carotenoid, cartilage, chondroprotection, ROS

Introduction

Osteoarthritis (OA) is a progressive degenerative joint disease associated with the gradual degradation of articular cartilage, remodeling of the subchondral bone, synovial inflammatory changes and changes in periarticular tissues (1). According to the Global Burden of Disease Study 2021, ~607 million individuals worldwide were living with OA in 2021, with an age-standardized prevalence rate of 6,967.3 per 100,000 population (2). OA remains one of the most common causes of disability worldwide and represents a major personal and socioeconomic burden; it presents significant barriers to healthcare, underscoring the need for intervention strategies that may alter the fundamental causes of the disease (3). OA is a condition characterized by sustained alterations in inflammatory signaling pathways, including increased levels of proinflammatory (such as IL-1β and IL-6) cytokines, matrix-degrading enzymes (such as MMP3, MMP13 and ADAMTS5) and oxidative stress, which disrupt the normal processes of cartilage synthesis and degradation (4). OA is considered to be a multimodal disease because of multilevel changes resulting from the interplay among the synovium, subchondral bone and cartilage (5).

Chondrocytes are resident cells of cartilage that are essential for maintaining cartilage homeostasis and contribute to OA pathogenesis. Pathological damage leads to inadequate

cartilage repair and disease progression (6). Chondrocytes produce inflammatory cytokines, such as IL-1β and IL-6, that have been implicated in aggravating OA by increasing MMP levels while inhibiting the endogenous inhibitors of MMP activity, thereby contributing to cartilage degradation (7-9). Current treatment options for OA, including physiotherapy, pharmacological agents and surgical interventions, mitigate pain and stiffness but do not promote cartilage restoration or halt disease progression (10). Consequently, these limitations have increased interest in novel therapies targeting the underlying molecular mechanisms of OA.

Fucoxanthin (FUC) is a carotenoid primarily derived from brown algae. In various disease models, including cancer, obesity, diabetes, liver fibrosis and intestinal inflammation, FUC has been shown to display anti-inflammatory, antioxidant and other bioactive activities (11-13). FUC may protect against inflammation by inhibiting the release of proinflammatory cytokines IL-6 and IL-1β, which are associated with the pathogenesis of OA (14,15). Furthermore, FUC has a nutraceutical potential, as it enhances cellular resistance to oxidative stress (11,12,16).

The anti-inflammatory effects of FUC have been demonstrated in various pathological conditions, such as acute lung injury, ulcerative colitis, rheumatoid arthritis, endometritis and drug-induced hepatotoxicity (17). Emerging evidence from OA-related models indicates the therapeutic potential of FUC (4,18). However, understanding how FUC modulates the inflammatory response in chondrocytes and contributes to cartilage homeostasis, potentially through the Janus kinase (JAK)2/STAT3 signaling pathway, a central mediator in OA pathogenesis (19), remains to be fully elucidated. Thus, the present study aimed to examine whether FUC can protect cartilage homeostasis in OA and determine whether its mechanism involves targeted regulation of the JAK2/STAT3 signaling axis.

Materials and methods

Animals models. All animal procedures were approved by the Animal Ethics Committee of Renmin Hospital of Wuhan University (approval no. 20230101A; Wuhan, China) and conducted in accordance with the National Institutes of Health Guide for the Care and Use of Laboratory Animals (20). This approval covered the use of both 6-week-old rats for the *in vivo* model and 6-day-old neonatal rats for primary chondrocyte isolation.

In the present study, two independent *in vivo* experiments were conducted using a total of 36 Sprague-Dawley (SD) rats (weight, 200-220 g), acquired from SPF Biotechnology Co., Ltd. All animals were specific pathogen free-grade and housed under controlled conditions (temperature 22±2˚C; relative humidity 45-65%; 12:12 h light-dark cycle) with ad libitum access to food and water. Following acclimation for 7 days, animals were randomly assigned to experimental groups. The first experiment involved 24 healthy 6-week-old male rats randomly divided into four groups (n=6 per group): Sham, anterior cruciate ligament transection (ACLT), ACLT + FUC (100 mg/kg) and ACLT + FUC (200 mg/kg). The second experiment consisted of 12 6-week-old male SD rats divided into two groups (n=6 per group): ACLT + FUC (200 mg/kg) and ACLT + FUC (200 mg/kg) + RO8191. OA was induced using the ACLT method. Specifically, rats were anesthetized with isoflurane (induction, 3.5%; maintenance, 1.5%) delivered in 100% oxygen at a flow rate of 1.0 l/min via a face mask. Anesthetic depth was continuously monitored through the toe pinch reflex and respiratory rate throughout the procedure. The knee joint was then exposed. The ACL was transected in the ACLT- and FUC-treated groups, while the sham group underwent joint cavity exposure without ligament transection. FUC (cat. no. HY-N2302; MedChemExpress), isolated from the diatom *Phaeodactylum tricornutum* with a chemical purity of >90% (confirmed by high-performance liquid chromatography), was prepared in corn oil. Corn oil was chosen as the vehicle because of the lipophilic properties of FUC. Beginning 1 week post-surgery, rats in the treatment groups received intra-articular injections of FUC (in a volume of 15 μl) every 3 days for a total of 7 weeks, while the sham and ACLT groups received an equal volume of corn oil. Before each intra-articular injection, rats were anesthetized using isoflurane. Anesthesia was induced with 3-5% isoflurane and 1-2 l/min oxygen; after loss of the righting reflex and muscle relaxation, anesthesia was maintained using a face mask delivering 1.5-2.5% isoflurane and 0.5-1 l/min oxygen. The doses of 100 and 200 mg/kg were selected based on a previous study demonstrating that FUC at this range exerts protective effects *in vivo* (21), as well as preliminary dose-finding experiments in the present study. For the RO8191 co-treatment group, RO8191 (5 μM; cat. no. HY-W063968; MedChemExpress) was co-administered with FUC via intra-articular injections at the same volume (15 μl per joint) every 3 days for 7 weeks. Histological analysis showed no indication of oil-induced inflammation (Fig. 1), suggesting that corn oil is acceptable for continuous intra-articular administration.

During the study, all animals were checked daily for any indication of distress. The following humane endpoints were set in advance: i) Weight loss of >20% of starting body weight for 2 consecutive days; ii) complete loss of weight-bearing on the operated leg or inability to reach food and water; iii) severe, ongoing knee swelling with skin ulcers or an infection that did not improve with treatment; iv) acute respiratory distress; v) consistently low body temperature or notably reduced heart rate; and vi) a critical, near-death condition. However, none of the 36 rats reached any of the predefined humane endpoints, and all animals were euthanized at the designated experimental endpoints in compliance with the approved animal protocol.

In total, 8 weeks post-surgery, rats were euthanized by cervical dislocation under deep anesthesia induced with 5% isoflurane (confirmed by the absence of pedal reflex), consistent with the American Veterinary Medical Association guidelines (22). Knee joints were harvested immediately.

Histopathological analysis. The cartilage tissues of rats were isolated and fixed in 4% paraformaldehyde for 48 h at 20˚C (room temperature), followed by dehydration using an ethanol gradient and immersion in paraffin. The samples were sectioned to a 4-μm thickness and stained using H&E or Safranin O-Fast Green. H&E staining was performed at 60˚=C for 6 min (hematoxylin) and at room temperature for 2 min (eosin). Safranin O-Fast Green staining was performed at room temperature for 8 min (hematoxylin) and

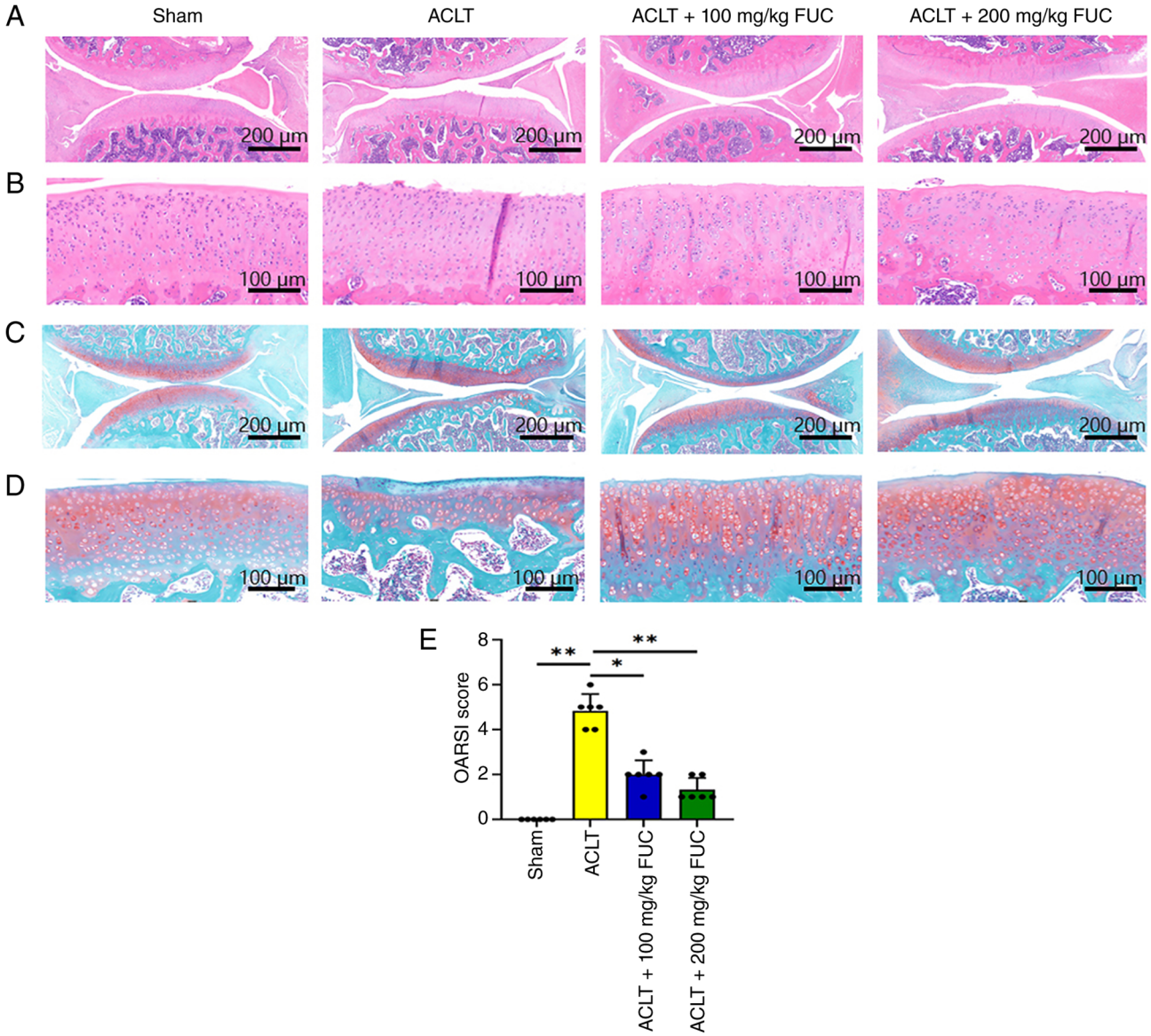

Figure 1. FUC prevents cartilage degradation in an ACLT-induced osteoarthritis model. Histological analysis of knee joints from male Sprague-Dawley rats harvested 8 weeks after ACLT surgery (n=6). Representative (A) full-joint coronal and (B) high-magnification H&E-stained sections of articular cartilage from the sham, ACLT and FUC-treated (100 and 200 mg/kg) groups. Representative (C) full-joint coronal and (D) high-magnification Safranin O-Fast Green-stained sections showing proteoglycan content. (E) OARSI scoring of full-joint coronal sections, with corresponding high-magnification views (n=6). Scale bars: 200 μm for (A,C) full-joint coronal sections; 100 μm for (B,D) high-magnification sections. Data are presented as the mean ± SD. *P<0.05; **P<0.01. ACLT, anterior cruciate ligament transection; FUC, fucoxanthin; OARSI, Osteoarthritis Research Society International.

4 min (Fast Green), and at 60˚C for 12 min (Safranin O). The Osteoarthritis Research Society International (OARSI) scoring system was utilized to measure the degree of cartilage degeneration (23). The sections were evaluated under an upright fluorescent microscope (BX51; Olympus Corporation) for histopathological changes. Histological scoring using the OARSI system was performed by observers blinded to the experimental groups.

Cell culture. Primary chondrocytes were isolated from the knee joints of 6-day-old newborn SD rats (both male and female; weight 12-18 g). The rats were anesthetized with 5% isoflurane in 1 l/min oxygen until loss of the righting reflex and absence of toe pinch response, followed by euthanasia by cervical dislocation. Immediately after euthanasia, bilateral knee joints were dissected under sterile conditions. Chondrocytes were cultured in DMEM/F12 (Wuhan Servicebio Technology Co., Ltd.) complete medium, supplemented with 10% FBS (Gibco; Thermo Fisher Scientific, Inc.), 100 IU/ml penicillin G and 100 μg/ml streptomycin (Wuhan Servicebio Technology Co., Ltd.). The cultures were maintained at 37˚C in a 5% CO_2 incubator. Cells were allowed to proliferate, and only second-passage chondrocytes were utilized for further experiments to ensure phenotypic stability. The chondrocyte phenotype was assessed by observing the cell shape during culture. All *in vitro* experiments were performed using biological replicates derived from independent chondrocyte isolations, and technical replicates were included when applicable. For RO8191 treatment, chondrocytes were co-incubated with 5 μM RO8191 together with IL-1β, FUC or both at 37˚C

in 5% CO_2 for 24 h. Recombinant rat IL-1β (cat. no. RP01788; ABclonal Biotech Co., Ltd.) was used for cell stimulation at a concentration of 10 ng/ml at 37˚C for 24 h. For control groups, untreated chondrocytes served as the negative control and IL-1β-only treated chondrocytes served as the model control.

Cytotoxicity and antioxidant capacity assay. The cytotoxic effects of FUC treatment on chondrocytes were analyzed using the Cell Counting Kit-8 (CCK-8; Beyotime Biotechnology) assay. Cells were placed in 96-well plates in a concentration of $5x10^3$ cells per well. Following attachment, FUC treatment was applied at concentrations of 0, 5, 10, 15, 20, 25 and 30 μM for 24, 48 and 72 h. The CCK-8 solution was added to each well at a volume of 10 μl and incubated at 37˚C for 2 h. After incubation, the absorbance was determined at 450 nm using a microplate reader (EnVision; PerkinElmer, Inc.).

In addition, the extracellular antioxidant activity of FUC was measured using a 2,2-diphenyl-1-picrylhydrazyl (DPPH) free radical scavenging assay (cat. no. A153-1; Nanjing Jiancheng Bioengineering Institute) and a hydroxyl radical (OH^-) assay (cat. no. A018-1; Nanjing Jiancheng Bioengineering Institute). FUC was tested at concentrations ranging from 0 to 30 μM. For the DPPH assay, the reaction mixture was incubated at room temperature (25˚C) in the dark for 30 min; for the hydroxyl radical-assay, the reaction mixture was incubated at room temperature (25˚C) in the dark for 20 min, according to the manufacturer protocols.

Reactive oxygen species (ROS) measurement. Chondrocytes were cultured in 6-well plates at 70% density under stimulation with IL-1β at a concentration of 10 ng/ml for 24 h. Following washing with PBS, cells were treated with serum-free DMEM/F12 containing 10 μM 2',7'-dichlorofluorescein diacetate (cat. no. S0033S; Beyotime Biotechnology) for 30 min at 20˚C. Images were captured via an inverted fluorescent microscope after washing out undesired probes with PBS. The average fluorescence intensity was calculated using ImageJ software (version 1.8.0; National Institutes of Health).

RNA preparation and reverse transcription-quantitative PCR (RT-qPCR) analysis. Chondrocytes were seeded in 6-well plates at a density of $3x10^5$ cells per well and cultured for 24 h. Total RNA extraction was performed using RNAeasy™ Animal RNA Extraction Kit (cat. no. R0026; Beyotime Biotechnology), and cDNA was synthesized by reverse transcription with SweScript RT I First Strand cDNA Synthesis Kit (cat. no. G3330; Wuhan Servicebio Technology Co., Ltd.) according to the manufacturer's instructions. The reverse transcription reaction was performed at 50˚C for 15-30 min, followed by inactivation at 85˚C for 5 sec. RT-qPCR was conducted with specific primers for each gene using the SYBR Green qPCR Master Mix (cat. no. G3320; Wuhan Servicebio Technology Co., Ltd.) on a real-time PCR system. The thermocycling conditions were: Initial denaturation at 95˚C for 30 sec, followed by 40 cycles of denaturation at 95˚C for 5 sec and combined annealing/extension at 60˚C for 30 sec. A melting curve analysis was performed after amplification to verify product specificity. Relative gene expression was calculated using the $2^{-\Delta\Delta Cq}$ method by normalizing the target mRNA levels to the levels of β-actin (24). The primer sequences used are presented in Table I.

Table I. Primer sequences used for reverse transcription-quantitative PCR analysis.

Gene	Sequence (5'-3')
IL6	F: AAATCTGCTCTGGTCTTC
	R: AGGGTTTCAGTATTGCTC
MMP3	F: GTCCAGAAGATCGATGCAGC
	R: TCCAACTGTGAAGATCCGCT
MMP13	F: GCCACCTTCTTCTTGTTGAGTTG
	R: GACTTCTTCAGGATTCCCGCA
ADAMTS5	F: ACAAGAGTCTGGAGGTGAGCAAG
	R: ACATATGGTCCCAACGTCTGC
β-actin	F: TGCTATGTTGCCCTAGACTTCG
	R: GTTGGCATAGAGGTCTTTACGG

ADAMTS, a disintegrin and metalloproteinase with thrombospondin motifs; F, forward; R, reverse.

Western blotting. Total cellular protein was extracted using RIPA buffer (cat. no. G2002; Wuhan Servicebio Technology Co., Ltd.) in combination with PMSF (cat. no. G2008; Wuhan Servicebio Technology Co., Ltd.), a phosphatase inhibitor (cat. no. G2007; Wuhan Servicebio Technology Co., Ltd.) and a 50X protease inhibitor cocktail (cat. no. G2006; Wuhan Servicebio Technology Co., Ltd.). The lysates were incubated on ice for 30 min before undergoing centrifugation for 10 min at 16,100 x g at 4˚C. The resulting supernatant was collected, and protein amount was quantified using the BCA Protein Assay Kit (cat. no. G2026; Wuhan Servicebio Technology Co., Ltd.). Proteins (30 μg per lane) were transferred to PVDF membranes after undergoing 12% SDS-PAGE. The membranes were incubated with primary antibodies overnight at 4˚C after they had been blocked with 5% skimmed milk (cat. no. GC310001; Wuhan Servicebio Technology Co., Ltd.) in TBS-Tween for 1 h at 20˚C, followed by incubation with primary antibodies overnight at 4˚C. The primary antibodies consisted of inducible nitric oxide synthase (iNOS; 1:1,000; cat. no. A14031; Abclonal Biotech Co., Ltd.), MMP3 (1:1,000; cat. no. A22328; ABclonal Biotech Co., Ltd.), MMP13 (1:1,000; cat. no. 18165-1; Proteintech Group, Inc.), cyclooxygenase-2 (COX-2; 1:1,000; cat. no. A1253; Abclonal Biotech Co., Ltd.), a disintegrin and metalloproteinase with thrombospondin motifs 5 (ADAMTS5; 1:1,000; cat. no. A2836; ABclonal Biotech Co., Ltd.), IL-6 (1:1,000; cat. no. CPA4914; Cohesion Biosciences), phosphorylated (p)-JAK2 (1:2,000; AP0531; cat. no. Abclonal Biotech Co., Ltd.), JAK2 (1:2,000; cat. no. A11497; Abclonal Biotech Co., Ltd.), β-actin (1:3,000; cat. no. GB11001; Wuhan Servicebio Technology Co., Ltd.), p-STAT3 (1:2,000; cat. no. T56566; Abmart Pharmaceutical Technology Co., Ltd.) and STAT3 (1:2,000; cat. no. T55292; Abmart Pharmaceutical Technology Co., Ltd.). The membranes were then incubated with HRP-conjugated goat anti-rabbit IgG secondary antibody (cat. no. GB23303; Wuhan Servicebio Technology Co., Ltd.) at a dilution of 1:10,000 for 1 h at room temperature. The protein signals were visualized with an ECL detection system (cat. no. G2020; Wuhan Servicebio Technology Co.,

Ltd.) on the ChemiDoc Touch imaging system (Bio-Rad Laboratories, Inc.). Images were assessed semi-quantitatively utilizing ImageJ software (version 1.8.0).

Immunofluorescence. Chondrocytes were cultured on glass coverslips for 24 h. After being fixed in 4% paraformaldehyde for 30 min at room temperature (20-25˚C), then permeabilized and blocked with 1% BSA (Beijing Solarbio Science & Technology Co., Ltd.) at room temperature for 60 min, followed by incubation at 4˚C overnight with an MMP3 antibody (1:400; cat. no. GB12131; Wuhan Servicebio Technology Co., Ltd.). Fluorescence labeling was assessed utilizing the Tyramide signal amplification staining kit (cat. no. G1236; Wuhan Servicebio Technology Co., Ltd.), and nuclei were visualized with DAPI staining, both according to the manufacturers' instructions. Fluorescence microscopy was used to analyze the chondrocytes. Quantification of fluorescence signal was performed utilizing ImageJ software (version 1.8.0).

ELISA. Following the manufacturer's instructions, 100 μl of cell culture supernatant was added to the wells of a 96-well microplate pre-coated with specific antibodies. Rat IL-6 ELISA Kit (cat. no. GER0001; Wuhan Servicebio Technology Co., Ltd.) and rat IL-1β ELISA Kit (cat. no. GER0002; Wuhan Servicebio Technology Co., Ltd.) were used to assess the amounts of cytokines in the supernatants. A standard curve was created according to the kit instructions, and the optical density values of the samples were used to quantify cytokine concentrations according to the standard curve.

Immunohistochemistry. Tissue fixation, paraffin embedding and sectioning were performed exactly as described in the histopathological analysis section. Prior to staining, 4-μm-thick sections were deparaffinized in three changes of xylene for 5 min each and rehydrated through a descending ethanol series (100% ethanol twice for 2 min, 95% ethanol twice for 2 min, 80% ethanol once for 2 min, 70% ethanol once for 2 min) followed by a final rinse in distilled water. Antigen retrieval was performed by heating sections in 0.01 M sodium citrate buffer (pH 6.0) at 95˚C for 20 min in a water bath, after which sections were allowed to cool naturally to room temperature. Endogenous peroxidase activity was quenched by incubation with 3% hydrogen peroxide in methanol at room temperature for 15 min. Non-specific binding was blocked with 3% BSA in phosphate-buffered saline containing 0.05% Tween-20 (PBS-T) at room temperature for 30 min. Tissue sections were then incubated overnight at 4˚C with primary antibodies against p-JAK2 (1:1,000; cat. no. AP0531; Abclonal Biotech Co., Ltd.), JAK2 (1:1,000; cat. no. A11497; Abclonal Biotech Co., Ltd.), p-STAT3 (1:1,000; cat. no. T56566; Abmart Pharmaceutical Technology Co., Ltd.) and STAT3 (1:1,000; cat. no. T55292; Abmart Pharmaceutical Technology Co., Ltd.). The antibody dilutions used for immunohistochemistry were identical to those used for western blotting. After three washes with PBS-T for 5 min each, sections were incubated with HRP-conjugated goat anti-rabbit IgG (1:2,000; cat. no. ab6721; Abcam) at 37˚C for 50 min. Immunoreactivity was visualized using 3,3'-diaminobenzidine (Dako; Agilent Technologies, Inc.) as the HRP substrate, followed by counterstaining with hematoxylin. Images of the stained sections were captured with an inverted microscope (NIKON ECLIPSE CI; Nikon Corporation), and the mean integral optical density was quantified using Image-Pro Plus Software (version 6.0; Media Cybernetics, Inc.).

Statistical analysis. Data are presented as the mean ± the standard deviation and were analyzed with SPSS 25.0 (IBM Corp.) and GraphPad Prism 8.0.2 (Dotmatics). Data normality was assessed using the Shapiro-Wilk test. Data having a normal distribution were analyzed using one-way ANOVA with Bonferroni's post hoc test, whereas non-normally distributed data were assessed using the Kruskal-Wallis H test followed by Dunn's post hoc test. $P<0.05$ was considered to indicate a statistically significant difference.

Results

FUC alleviates ACLT-induced OA. To evaluate the structural effects of FUC on OA progression *in vivo*, an ACLT-induced OA rat model was established. Histological evolution of full-joint coronal sections (Fig. 1A and C), with corresponding high-magnification images (Fig. 1B and D), obtained 8 weeks after surgery showed marked differences among the experimental groups.

In the H&E-stained sections, cartilage from the sham group showed a smooth and continuous articular surface with a regular layer of chondrocytes (Fig. 1A and B). By contrast, the ACLT group showed evident cartilage degeneration, characterized by surface fibrillation and erosion, decreased chondrocyte density and disruption of the subchondral bone plate (Fig. 1A and B). FUC treatment exerted a dose-dependent protective effect. The ACLT + 100 mg/kg FUC group showed partial cartilage preservation with less surface disruption, whereas the ACLT + 200 mg/kg FUC group retained nearly normal cartilage morphology, tidemark integrity and cellular architecture, similar to those observed in the sham group (Fig. 1A and B).

Safranin O-Fast Green staining supported these findings by demonstrating alterations in proteoglycan content. Depletion of Safranin O staining, indicative of proteoglycan loss was observed in the ACLT group (Fig. 1C and D), which was ameliorated by FUC treatment in a dose-dependent manner, with the 200 mg/kg FUC group demonstrating strong, homogeneous Safranin O staining throughout the articular cartilage (Fig. 1C and D).

Quantitative evaluation using the OARSI histopathology system confirmed these findings. The OARSI scores were significantly higher in the ACLT group than in the sham group (Fig. 1E; $P<0.01$). FUC treatment significantly decreased OARSI scores in a dose-dependent manner; both the 100 and 200 mg/kg FUC groups showed lower scores than those in the ACLT group (Fig. 1E; $P<0.05$), with the greatest reduction observed in the 200 mg/kg group (Fig. 1E; $P<0.01$).

Collectively, these results suggested that intra-articular administration of FUC effectively attenuates ACLT-induced cartilage degradation, preserves proteoglycan content, and maintains joint structural integrity in a dose-dependent manner.

FUC significantly enhances the antioxidant capacity of chondrocytes. After demonstrating the cartilage-protective effects of FUC *in vivo*, its direct cytoprotective effects on articular chondrocytes were evaluated *in vitro*. The chemical structure of FUC is shown in Fig. 2A. To determine the safe and effective concentration range, chondrocyte viability was measured following FUC treatment using the CCK-8 assay (Fig. 2B). CCK-8 analysis showed that FUC at concentrations between 5 and 15 μM maintained chondrocyte viability at 24, 48 and 72 h compared with untreated controls, whereas concentrations ≥20 μM resulted in a significant reduction in cell viability ($P<0.05$), indicating cytotoxic effects at higher doses (Fig. 2B).

Hydroxyl radical- and DPPH-scavenging assays were performed to evaluate the antioxidant capacity of FUC. FUC demonstrated considerable free-radical scavenging activity in a dose-dependent manner, with maximal inhibition at ~15 μM (Fig. 2C; $P<0.01$). Given its optimal antioxidant potential and promising safety profile, a 15 μM FUC dose was selected for subsequent experiments.

Next, it was investigated whether FUC could alleviate inflammation-induced oxidative stress in chondrocytes. Fluorescence imaging showed that IL-1β stimulation significantly elevated intracellular ROS levels compared with those in the negative control (NC) group (Fig. 2D; $P<0.01$). Quantitative analysis of fluorescence intensity showed that FUC co-treatment attenuated IL-1β-induced ROS levels (Fig. 2D; $P<0.05$). These results suggested that FUC protects chondrocytes from inflammation-induced oxidative stress.

FUC exhibits anti-inflammatory effects in chondrocytes treated with IL-1β. Subsequently, it was examined whether the cytoprotective effects of FUC extend to the modulation of OA-associated inflammation and cartilage catabolism in chondrocytes. In IL-1β-stimulated chondrocytes, FUC co-treatment significantly attenuated the upregulation of key inflammatory and catabolic markers.

At the transcriptional level, RT-qPCR analysis showed that IL-1β stimulation significantly increased the mRNA expression of IL-6, MMP3, MMP13 and ADAMTS5 compared with that in the NC group (Fig. 3A; $P<0.01$). FUC co-treatment significantly reduced the IL-1β-induced expression of these genes (Fig. 3A; $P<0.05$).

Consistent with the transcriptional findings, western blot analysis demonstrated that IL-1β markedly increased the protein expression levels of IL-6, COX-2, iNOS, MMP3, MMP13 and ADAMTS5 compared with that in controls (Fig. 3B; $P<0.05$). Treatment with FUC significantly suppressed the IL-1β-induced upregulation of COX-2, MMP3, MMP13 and ADAMTS (Fig. 3B; $P<0.05$), whereas the suppression of IL-6 and iNOS did not reach statistical significance (Fig. 3B).

Furthermore, immunofluorescence staining revealed a pronounced increase in MMP3 expression in IL-1β-treated chondrocytes compared with that in the NC group (Fig. 3C; $P<0.01$). This increase was significantly attenuated by co-treatment with FUC (Fig. 3C; $P<0.05$).

Collectively, these results demonstrated that FUC suppresses IL-1β-induced inflammatory and catabolic responses in chondrocytes.

FUC-mediated chondroprotection is associated with the JAK2/STAT3 signaling cascade. Based on the observed chondroprotective effects of FUC, it was investigated whether these effects were associated with inhibition of the JAK2/STAT3 signaling pathway *in vivo*. Given the central role of JAK2/STAT3 signaling in OA-associated inflammation and cartilage catabolism (19), a gain-of-function approach was employed to assess pathway involvement.

Rats with ACLT-induced OA were treated with 200 mg/kg FUC either alone or in combination with the JAK2/STAT3 activator RO8191. Histological assessment of full-joint coronal sections (Fig. 4A and C), with corresponding high-magnification views (Fig. 4B and D), revealed marked differences between the treatment groups.

H&E staining showed that FUC treatment alone maintained cartilage integrity, as evidenced by a smooth articular surface, intact tidemark and well-aligned distribution of chondrocytes in the femoral condyle and tibial plateau (Fig. 4A and B). By contrast, co-administration of RO8191 significantly impaired these protective effects, as evidenced by surface irregularities, cartilage thinning and chondrocyte disorganization (Fig. 4A and B).

Cartilage from FUC-treated joints exhibited intense and homogeneous Safranin O staining, suggesting retention of proteoglycan content (Fig. 4C and D); however, co-treatment with RO8191 resulted in proteoglycan loss and matrix depletion, especially in weight-bearing areas of the joint (Fig. 4C and D).

Quantitative evaluation using the OARSI histopathology scoring system confirmed these findings. OARSI scores were significantly higher in the FUC + RO8191 group than in the FUC-alone group (Fig. 4E; $P<0.01$), indicating that activation of JAK2/STAT3 signaling significantly attenuated the cartilage-protective effects of FUC.

To directly determine whether FUC modulates JAK2/STAT3 signaling *in vivo*, immunohistochemical staining for p-JAK2, p-STAT3 and their total forms was performed on articular cartilage sections (Fig. 4F). Cartilage from rats treated with FUC + RO8191 showed significantly increased p-JAK2 and p-STAT3 immunoreactivity compared with that from rats treated with FUC alone (Fig. 4F; $P<0.01$). Total JAK2 and STAT3 expression levels were comparable between groups.

Collectively, these results support the interpretation that the *in vivo* chondroprotective effects of FUC are associated with suppression of the JAK2/STAT3 signaling pathway, as pharmacological activation of this pathway significantly reversed the beneficial effects of FUC on cartilage integrity.

FUC reduces inflammation with involvement of the JAK2/STAT3 signaling pathway. To investigate whether the anti-inflammatory effects of FUC in IL-1β-stimulated chondrocytes were associated with regulation of the JAK2/STAT3 signaling pathway, the protein expression of total, p-JAK2 and p-STAT3 was analyzed. Western blot analysis showed that IL-1β stimulation significantly increased JAK2 and STAT3 phosphorylation levels compared with those in the NC group (Fig. 5A; $P<0.01$), accompanied by increased protein expression of iNOS, IL-6, MMP3 and MMP13 (

. 5A; $P<0.05$). FUC co-treatment significantly reduced JAK2 and STAT3 phosphorylation levels (Fig. 5A; $P<0.05$) and downregulated these inflammatory and catabolic proteins (Fig. 5A;

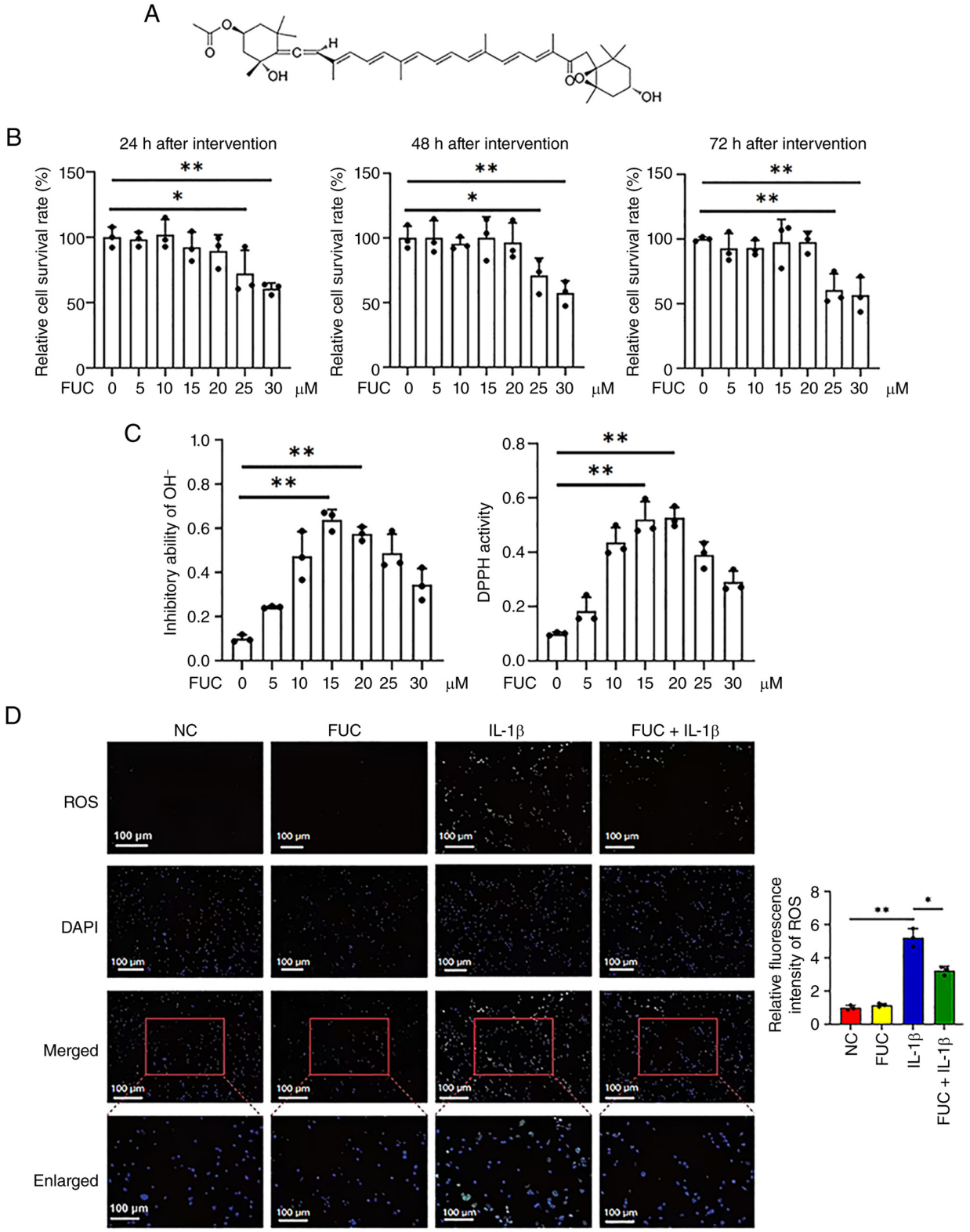

Figure 2. FUC enhances chondrocyte viability and inhibits oxidative stress *in vitro*. (A) Chemical structure of FUC. (B) Viability of primary rat chondrocytes treated with FUC (0-30 μM) for 24, 48 and 72 h, assessed by the Cell Counting Kit-8 assay. (C) *In vitro* antioxidant capacity of FUC measured by hydroxyl radical (OH^-) inhibition and DPPH radical scavenging assays. (D) Intracellular ROS levels measured by fluorescence microscopy in chondrocytes stimulated with or without IL-1β (10 ng/ml, 24 h) and co-treated with FUC (15 μM). Representative images, merged channels, enlarged views and quantitative fluorescence intensity analysis are shown. Scale bar, 100 μm. Data are presented as the mean ± SD from three independent experiments. *P<0.05; **P<0.01. NC, negative control; ROS, reactive oxygen species; FUC, fucoxanthin; DPPH, 2,2-diphenyl-1-picrylhydrazyl.

P<0.05); however, the downregulation of MMP13 did not reach statistical significance (Fig. 5A). Co-treatment with the JAK2 activator RO8191 significantly reversed the inhibitory effects of FUC on IL-6, MMP3 and MMP13 (Fig. 5A; P<0.05); however, the restoration of iNOS levels was not statistically significant (Fig. 5A).

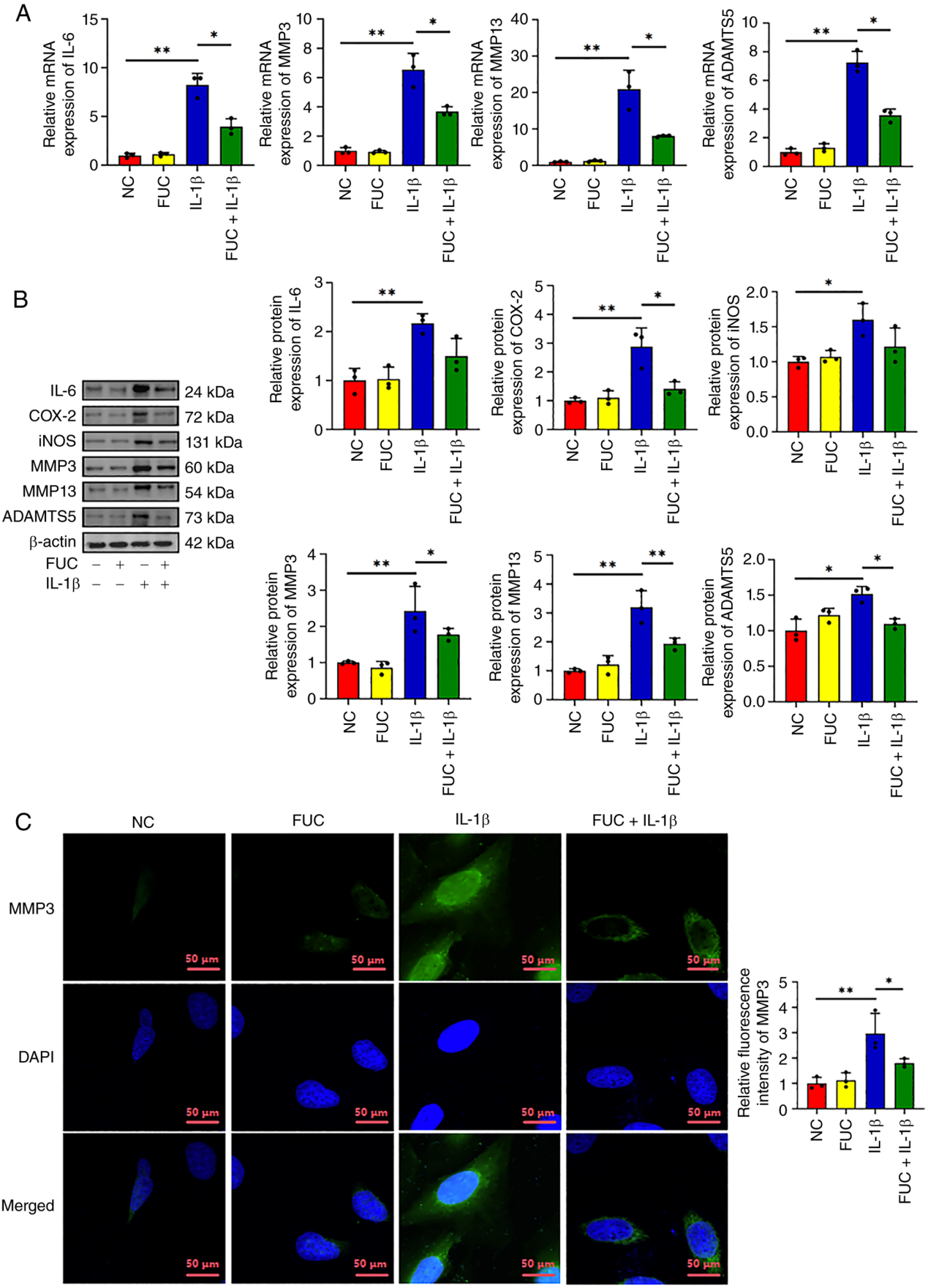

Figure 3. FUC exhibits anti-inflammatory effects in IL-1β-treated chondrocytes. (A) Reverse transcription-quantitative PCR analysis of IL-6, MMP3, MMP13 and ADAMTS5 (n=3). (B) Western blot and semi-quantitative analysis of inflammatory and catabolic protein expression in primary rat chondrocytes stimulated with IL-1β (10 ng/ml, 24 h) and co-treated with FUC (15 μM) (n=3). (C) Immunofluorescence staining of MMP3 in chondrocytes with nuclei labeled with DAPI. Scale bar, 50 μm. Data are presented as the mean ± SD. *P<0.05; **P<0.01. NC, negative control; FUC, fucoxanthin; ADAMTS, a disintegrin and metalloproteinase with thrombospondin motifs; COX-2, cyclooxygenase-2; iNOS, inducible nitric oxide synthase.

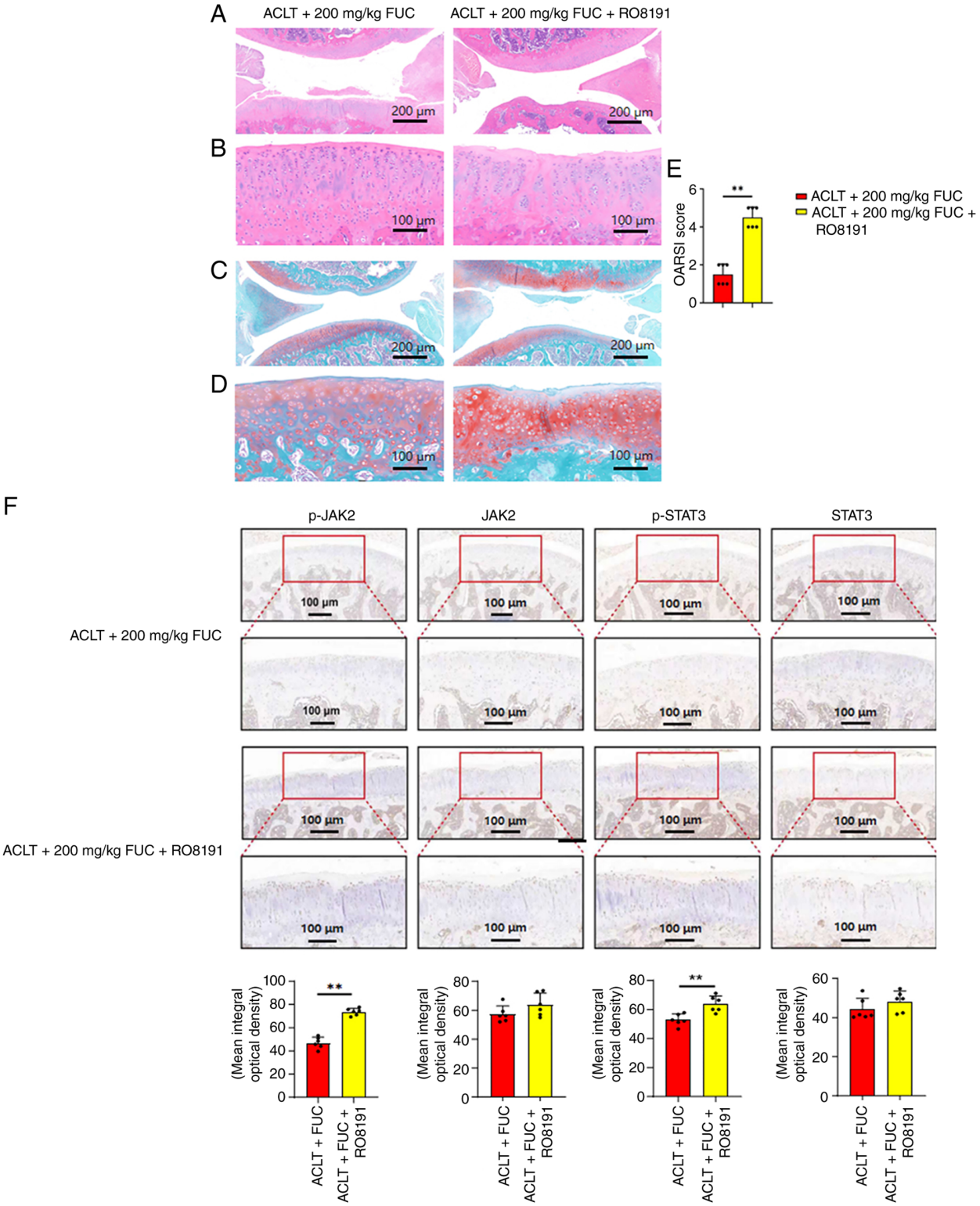

Figure 4. Effects of FUC and RO8191 on cartilage degeneration and JAK2/STAT3 signaling *in vivo*. Representative (A) H&E-stained full-joint coronal sections and (B) corresponding high-magnification images of articular cartilage from ACLT rats treated with 200 mg/kg FUC, with or without RO8191 (n=6). Representative (C) Safranin O-Fast Green-stained full-joint coronal sections and (D) corresponding high-magnification images showing cartilage proteoglycan content (n=6). (E) OARSI scores of full-joint coronal sections, with corresponding high-magnification views (n=6). (F) Immunohistochemical staining and quantitative analysis of p-JAK2, total JAK2, p-STAT3 and total STAT3 in articular cartilage (n=6). Scale barrs: 200 μm for (A,C) full-joint coronal sections; 100 μm for (B,D) high-magnification sections. Data are presented as the mean ± SD. **P<0.01. ACLT, anterior cruciate ligament transection; FUC, fucoxanthin; OARSI, Osteoarthritis Research Society International; p, phosphorylated; JAK, Janus kinase.

RT-qPCR analysis demonstrated that IL-1β significantly upregulated the mRNA expression of IL-6, MMP3, MMP13 and ADAMTS5 compared with that in the NC group (Fig. 5B; P<0.01). FUC treatment significantly suppressed the IL-1β-induced increases in these transcripts (Fig. 5B; P<0.05), whereas co-treatment with RO8191 significantly attenuated the

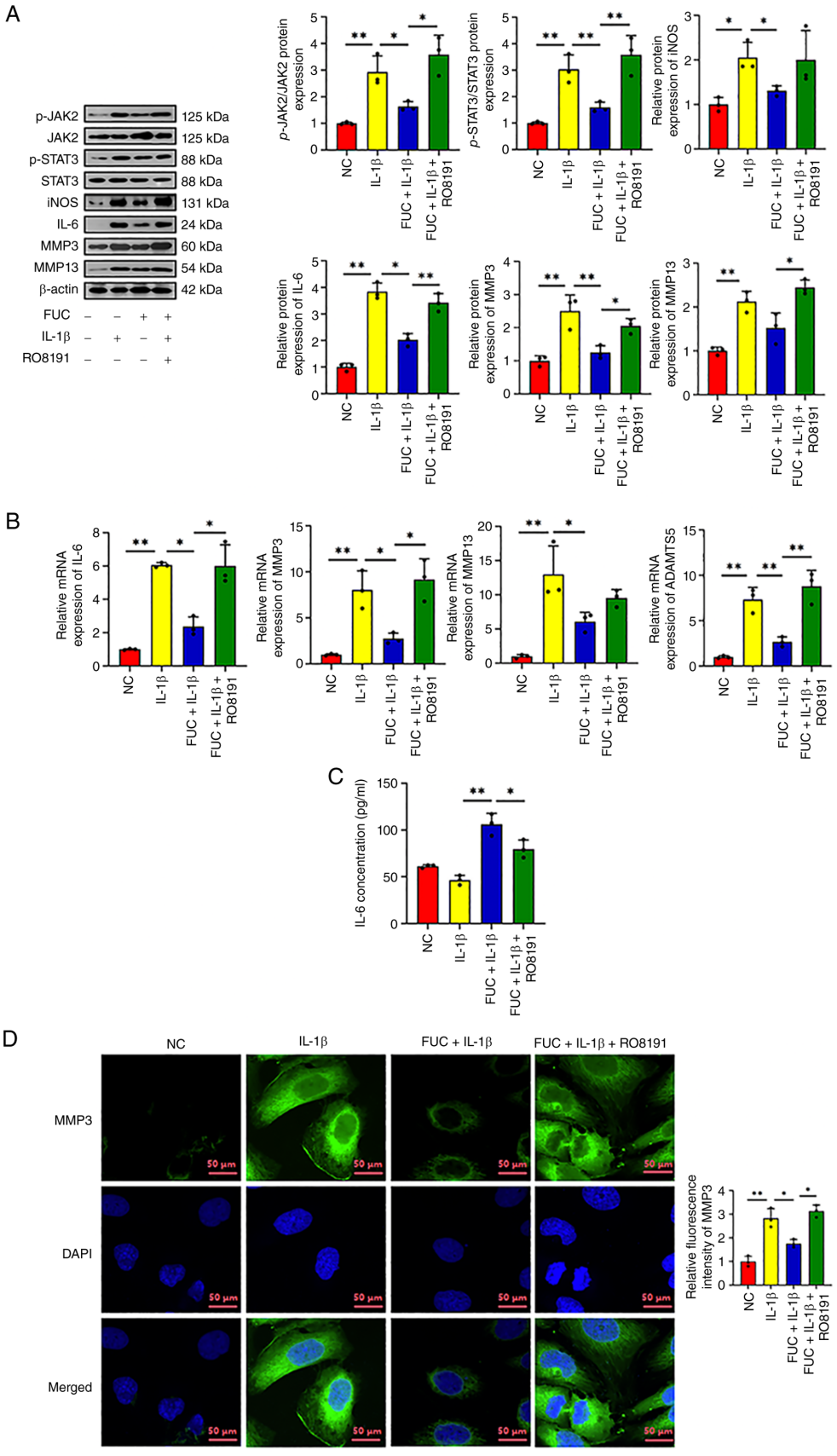

Figure 5. FUC reduces inflammatory responses associated with JAK2/STAT3 signaling *in vitro*. Primary rat chondrocytes were stimulated with IL-1β (10 ng/ml, 24 h) and treated with FUC (15 μM) and/or the JAK2 activator RO8191. (A) Western blot analysis and semi-quantitative evaluation of JAK2/STAT3 signaling components and inflammatory/catabolic protein expression (n=3). (B) Reverse transcription-quantitative PCR analysis of IL-6, MMP3, MMP13 and ADAMTS5 (n=3). (C) ELISA analysis of IL-6 secretion. (D) Immunofluorescence staining of MMP3 in chondrocytes with nuclei counterstained with DAPI, and corresponding quantitative fluorescence intensity analysis. Scale bar, 50 μm. Data are presented as the mean ± SD. *P<0.05; **P<0.01. NC, negative control; FUC, fucoxanthin; ADAMTS, a disintegrin and metalloproteinase with thrombospondin motifs; iNOS, inducible nitric oxide synthase; p, phosphorylated; JAK, Janus kinase.

suppressive effects of FUC on IL-6, MMP3 and ADAMTS5 (Fig. 5B; P<0.05); however, the restoration of MMP13 levels was not statistically significant (Fig. 5B).

Consistently, IL-1β stimulation significantly increased the ELISA-measured IL-6 protein levels compared with those in controls (Fig. 5C; P<0.01). These increases were significantly reduced by FUC treatment (Fig. 5C; P<0.05) and were partially restored by RO8191 co-treatment (Fig. 5C; P<0.05).

Furthermore, immunofluorescence staining revealed a marked increase in MMP3 expression in IL-1β-treated chondrocytes compared with that in the NC group (Fig. 5D; P<0.01). FUC treatment significantly reduced MMP3 fluorescence intensity (Fig. 5D; P<0.05), and this reduction was reversed by co-treatment with RO8191 (Fig. 5D; P<0.05).

Collectively, these findings suggested that FUC suppresses IL-1β-induced inflammatory responses, in part, through inhibition of JAK2/STAT3 signaling.

Discussion

OA is the most prevalent type of arthritis worldwide and a leading cause of chronic pain and disability (25). Despite ongoing research, OA pathogenesis remains poorly understood and involves a complex interplay of metabolic, inflammatory and biomechanical factors (26). Currently available medications, such as non-steroidal anti-inflammatory drugs and corticosteroids, are effective in managing pain and inflammation (25) but do not alter disease progression. Their clinical use is constrained by adverse effects, such as gastrointestinal toxicity, hematological effects, anaphylaxis and other hypersensitivity reactions (27). Critically, no currently available therapy prevents the progressive loss of articular cartilage (1,10). The continuing absence of disease-modifying OA drugs underscores the need for novel, safe agents that can protect joint structures.

The present study showed that FUC considerably attenuated cartilage destruction in an ACLT-induced OA rat model and protected chondrocytes from IL-1β-induced inflammatory and oxidative damage *in vitro*. A key mechanistic finding was that these effects were associated, at least in part, with suppression of the JAK2/STAT3 pathway.

This observation has substantial therapeutic implications. Unlike existing clinical drugs that generally offer symptomatic relief, the current results suggest that FUC provides direct chondroprotection. In the ACLT model, FUC treatment considerably reduced inflammatory markers, preserved cartilage architecture and reduced extracellular matrix degradation. This shift from symptom management toward structural preservation suggests that FUC may have disease-modifying potential; however, further studies are required to confirm this.

FUC, a carotenoid of marine origin, has various beneficial effects, including antioxidant, anti-inflammatory and anticancer properties (14,28). FUC has been previously demonstrated to modulate inflammatory signaling by inhibiting signaling pathways, including NF-κB and MAPK, resulting in decreased levels of proinflammatory cytokines, such as IL-6, IL-1β and TNF-α (17). Other studies have indicated the capacity of FUC to activate nuclear factor erythroid 2-related factor 2 through PI3K/AKT signaling (29) and to inhibit the toll-like receptor 4/myeloid differentiation primary response 88/NF-κB axis, thereby decreasing inflammation and oxidative stress (30). Although recent studies have examined FUC under OA conditions, showing reduced inflammation and matrix degradation in chondrocytes and joint tissues (4,18), the precise mechanisms underlying its cartilage-protective effects remain incompletely understood. Collectively, these findings suggest that FUC exerts its biological effects through multiple interconnected signaling pathways. In this context, the findings of the present study indicated that inhibition of JAK2/STAT3 signaling represents one pathway contributing to the observed effects of FUC, while the involvement of additional pathways, such as NF-κB, MAPK and PI3K/AKT cannot be excluded. Further studies are required to clarify the relative contributions and potential crosstalk between these pathways in OA.

The effective *in vitro* concentration of FUC was 15 μM (~10 μg/ml). Intra-articular injection of 200 mg/kg FUC in 15 μl results in an initial total local concentration of ~200-400 μg/ml. Although this total concentration is substantially higher than the *in vitro* effective concentration, the free (unbound) concentration available to chondrocytes is likely much lower due to protein binding in the synovial fluid. After accounting for protein binding, tissue penetration barriers, and drug clearance over the 3-day dosing interval, the estimated free concentration becomes comparable to the effective *in vitro* concentration. Therefore, the higher administered dose is necessary to achieve therapeutic levels within the joint.

The antioxidant action of FUC is attributed to its chemical structure, which includes conjugated double bonds that neutralize ROS and stabilize free radicals (13,31-33). Oxidative stress induces chondrocyte death and cartilage degradation in OA (34). Consistent with earlier findings showing that FUC attenuates H_2O_2-induced oxidative damage (35,36), the present study confirmed that FUC significantly inhibits IL-1β-mediated ROS accumulation in chondrocytes. These ROS-scavenging and anti-inflammatory effects indicate that FUC is a multitarget agent with notable therapeutic potential for OA.

It was also found that FUC strongly inhibited IL-1β-induced upregulation of prominent catabolic enzymes, including MMP-3, MMP-13 and ADAMTS-5, as well as the inflammatory cytokine IL-6 in chondrocytes. Reduced protein levels of MMP-3, as visualized by immunofluorescence, further supported the role of FUC in protecting extracellular matrix integrity. These results are consistent with the aforementioned previous reports and suggest that FUC interferes with essential degradative processes involved in OA progression.

The JAK2/STAT3 pathway plays a key role in inducing inflammation and cartilage breakdown in OA (19). In the present study, FUC treatment reduced IL-1β-induced phosphorylation of JAK2 and STAT3 without affecting total protein expression levels, suggesting that the pathway is modulated by FUC. Pharmacological activation of JAK2/STAT3 signaling using the agonist RO8191 attenuated the cytoprotective effects of FUC both *in vitro* and *in vivo*. Immunohistochemical assessment confirmed induction of JAK2 and STAT3 phosphorylation in joint tissues following co-treatment with FUC + RO8191 compared with the FUC-alone group, with a consequent loss

of cartilage protection. Collectively, these results support the interpretation that inhibition of the JAK2/STAT3 pathway contributes to the anti-inflammatory and chondroprotective effects of FUC.

The present *in vivo* findings support a potential therapeutic role for FUC. In an ACLT-induced OA rat model, administration of 200 mg/kg FUC improved cartilage morphology and restored proteoglycan levels to a near-normal range, consistent with reports of FUC enhancing cartilage integrity (4,18). These findings suggest that FUC may exert disease-modifying effects by preserving cartilage structure.

Although the current results are promising, several important limitations should be considered. The ACLT model is commonly utilized to study OA; however, evaluating FUC in additional models and over longer durations may better define its long-term efficacy and safety profile. Although JAK2/STAT3 inhibition appears central, the potential effects of FUC on other pathways, such as NF-κB or MAPK, have not yet been investigated and require further study. Despite the low oral bioavailability of FUC, reported to be as low as 0.06% in rats (37), intra-articular administration minimizes this limitation by enabling direct delivery to the joint cavity. The pharmacokinetic profile of FUC within the joint cavity, including its retention, distribution and clearance after intra-articular administration, has not yet been fully characterized. Although intra-articular delivery may improve localized exposure, quantitative evaluation of intra-articular drug concentrations is necessary. Future research should focus on defining pharmacokinetic parameters and optimizing dose translation. Novel formulation strategies, such as nanocarriers and structural modification, may also be useful in improving the pharmacokinetic profile of FUC (32,38-42). Further studies are required to determine the optimal dosing, route of administration and long-term safety in humans.

In conclusion, the present study explored the therapeutic potential and mechanism of action of FUC in OA. The findings indicated that FUC alleviates OA by preserving cartilage tissue, downregulating the production of proinflammatory cytokines, and inhibiting inflammation-induced oxidative stress, partially, through inhibition of the JAK2/STAT3 signaling pathway. Therefore, FUC may be a potential therapeutic candidate for OA, and warrants further investigation.

Acknowledgements

The authors would like to thank to Mrs Lina Zhou, Mrs Yingxia Jin, Mrs Lili Li and Mrs Yuan He (Central Laboratory, Renmin Hospital of Wuhan University) for their technical guidance and instruction during the experimental procedures.

Funding

This research was funded by the National Natural Science Foundation of China (grant no. 82372489), the Wuhan University Education and Development Foundation (grant no. 2002330), the Fundamental Research Funds for the Central Universities (grant no. 2042023kf0224) and the Cross-Innovation Talent Program of Renmin Hospital of Wuhan University (grant no. JCRCFZ2022-019).

Availability of data and materials

The data generated in the present study may be requested from the corresponding author.

Authors' contributions

MSA conceptualized the study, reviewed and edited the manuscript and contributed to developing the methodology and performing the experiments. HZ and XR contributed to study design and data acquisition. YZ developed the methods and analyzed the data. PZ conceived and supervised the study, wrote the original draft, and acquired funding. MSA and PZ confirm the authenticity of all the raw data. All authors read and approved the final manuscript.

Ethics approval and consent to participate

All animal experiments were approved by the Animal Ethics Committee of Renmin Hospital of Wuhan University (approval no. 20230101A) and conducted in accordance with institutional and national guidelines for animal care.

Patient consent for publication

Not applicable.

Competing interests

The authors declare that they have no competing interests.

References

1. Fox SM: Osteoarthritis: The disease. Multimodal management of canine osteoarthritis. CRC Press, Boca Raton, FL, pp23-39, 2016.
2. Wang Z, Xiao Z, Sun C, Xu G and He J: Global, regional and national burden of osteoarthritis in 1990-2021: A systematic analysis of the global burden of disease study 2021. BMC Musculoskelet Disord 25: 1021, 2024.
3. Al-Worafi YM: Osteoarthritis management in developing countries. Handbook of medical and health sciences in developing countries: Education, practice, and research. Springer, London, pp1-26, 2024.
4. Lee H, Jang H, Heo D, Eom JI, Han CH, Kim SM, Shin YS, Pan CH and Yang S: *Tisochrysis lutea* fucoxanthin suppresses NF-κB, JNK, and p38-associated MMP expression in arthritis pathogenesis via antioxidant activity. Antioxidants (Basel) 13: 941, 2024.
5. Primorac D, Molnar V, Rod E, Jeleč Ž, Čukelj F, Matišić V, Vrdoljak T, Hudetz D, Hajsok H and Borić I: Knee osteoarthritis: A review of pathogenesis and state-of-the-art non-operative therapeutic considerations. Genes (Basel) 11: 854, 2020.
6. Akkiraju H and Nohe A: Role of chondrocytes in cartilage formation, progression of osteoarthritis and cartilage regeneration. J Dev Biol 3: 177-192, 2015.
7. Kapoor M, Martel-Pelletier J, Lajeunesse D, Pelletier JP and Fahmi H: Role of proinflammatory cytokines in the pathophysiology of osteoarthritis. Nat Rev Rheumatol 7: 33-42, 2011.
8. Choy E, Isenberg D, Garrood T, Farrow S, Ioannou Y, Bird H, Cheung N, Williams B, Hazleman B, Price R, *et al*: Therapeutic benefit of blocking interleukin-6 activity with an anti-interleukin-6 receptor monoclonal antibody in rheumatoid arthritis: A randomized, double-blind, placebo-controlled, dose-escalation trial. Arthritis Rheum 46: 3143-3150, 2002.
9. Kostoulas G, Lang A, Nagase H and Baici A: Stimulation of angiogenesis through cathepsin B inactivation of the tissue inhibitors of matrix metalloproteinases. FEBS Lett 455: 286-290, 1999.
10. Adam MS, Zhuang H, Ren X, Zhang Y and Zhou P: The metabolic characteristics and changes of chondrocytes in vivo and in vitro in osteoarthritis. Front Endocrinol (Lausanne) 15: 1393550, 2024.

11. Peng J, Yuan JP, Wu CF and Wang JH: Fucoxanthin, a marine carotenoid present in brown seaweeds and diatoms: Metabolism and bioactivities relevant to human health. Mar Drugs 9: 1806-1828, 2011.
12. Xiao H, Zhao J, Fang C, Cao Q, Xing M, Li X, Hou J, Ji A and Song S: Advances in studies on the pharmacological activities of fucoxanthin. Mar Drugs 18: 634, 2020.
13. Zhang H, Tang Y, Zhang Y, Zhang S, Qu J, Wang X, Kong R, Han C and Liu Z: Fucoxanthin: A promising medicinal and nutritional ingredient. Evid Based Complement Alternat Med 2015: 723515, 2015.
14. Xu HY, Jiang MT, Yang YF, Huang Y, Yang WD, Li HY and Wang X: Microalgae-based fucoxanthin attenuates rheumatoid arthritis by targeting the JAK-STAT signaling pathway and gut microbiota. J Agric Food Chem 73: 11708-11719, 2025.
15. Lee AH, Shin HY, Park JH, Koo SY, Kim SM and Yang SH: Fucoxanthin from microalgae *Phaeodactylum tricornutum* inhibits pro-inflammatory cytokines by regulating both NF-κB and NLRP3 inflammasome activation. Sci Rep 11: 543, 2021.
16. Méresse S, Fodil M, Fleury F and Chénais BJ: Fucoxanthin, a marine-derived carotenoid from brown seaweeds and microalgae: A promising bioactive compound for cancer therapy. Int J Mol Sci 21: 9273, 2020.
17. Guan B, Chen K, Tong Z, Chen L, Chen Q and Su J: Advances in fucoxanthin research for the prevention and treatment of inflammation-related diseases. Nutrients 14: 4768, 2022.
18. Sorasitthiyanukarn FN, Muangnoi C, Haworth IS, Rojsitthisak P and Rojsitthisak P: Enhancement of anti-inflammatory activity of fucoxanthin through encapsulation in alginate/chitosan nanoparticles for potential osteoarthritis treatment. Int J Biol Macromol 318: 144873, 2025.
19. Chen B, Ning K, Sun ML and Zhang XA: Regulation and therapy, the role of JAK2/STAT3 signaling pathway in OA: A systematic review. Cell Commun Signal 21: 67, 2023.
20. Care IoLARCo, Animals UoL. Guide for the care and use of laboratory animals: US Department of Health and Human Services, Public Health Service, National, 1986.
21. Chen Y, Dong J, Gong L, Hong Y, Hu C, Bao Y, Chen H, Liu L, Huang L, Zhao Y, *et al*: Fucoxanthin, a marine derived carotenoid, attenuates surgery-induced cognitive impairments via activating Akt and ERK pathways in aged mice. Phytomedicine 120: 155043, 2023.
22. Leary S, Underwood W, Anthony R, Cartner S, Grandin T, Greenacre C, Gwaltney-Brant S, Ann McCrackin M, Meyer R, Miller D, *et al*: AVMA Guidelines for the Euthanasia of Animals, 2020 edition, 2020.
23. McAlindon TJ: Osteoarthritis research society international (OARSI) Classification and Guidelines. HSS J 8: 66-67, 2012.
24. Livak KJ and Schmittgen TD: Analysis of relative gene expression data using real-time quantitative PCR and the 2(-Delta Delta C(T)) method. Methods 25: 402-408, 2001.
25. Neogi T: The epidemiology and impact of pain in osteoarthritis. Osteoarthritis Cartilage 21: 1145-1153, 2013.
26. Li G, Liu S, Chen Y, Zhao J, Xu H, Weng J, Yu F, Xiong A, Uddutula A, Wang D, *et al*: An injectable liposome-anchored teriparatide incorporated gallic acid-grafted gelatin hydrogel for osteoarthritis treatment. Nat Commun 14: 3159, 2023.
27. Xu X, Lv H, Li X, Su H, Zhang X and Yang JJ: Danshen attenuates cartilage injuries in osteoarthritis in vivo and in vitro by activating JAK2/STAT3 and AKT pathways. Exp Anim 67: 127-137, 2018.
28. Gong B, Ma S, Yan Y and Wang ZJ: Progress on the biological characteristics and physiological activities of fucoxanthin produced by marine microalgae. Front Mar Sci 11: 1357425, 2024.
29. Kim MB, Kang H, Li Y, Park YK and Lee J: Fucoxanthin inhibits lipopolysaccharide-induced inflammation and oxidative stress by activating nuclear factor E2-related factor 2 via the phosphatidylinositol 3-kinase/AKT pathway in macrophages. Eur J Nutr 60: 3315-3324, 2021.
30. Li X, Huang R, Liu K, Li M, Luo H, Cui L, Huang L and Luo L: Fucoxanthin attenuates LPS-induced acute lung injury via inhibition of the TLR4/MyD88 signaling axis. Aging (Albany NY) 13: 2655-2667, 2020.
31. Mumu M, Das A, Emran TB, Mitra S, Islam F, Roy A, Karim MM, Das R, Park MN, Chandran D, *et al*: Fucoxanthin: A promising phytochemical on diverse pharmacological targets. Front Pharmacol 13: 929442, 2022.
32. Yuan Y, Ma M and Zhang SJFC: Recent advances in delivery systems of fucoxanthin. Food Chem 404: 134685, 2023.
33. Din NAS, Mohd Alayudin AS, Sofian-Seng NS, Rahman HA, Mohd Razali NS, Lim SJ and Wan Mustapha WA: Brown algae as functional food source of fucoxanthin: A review. Foods 11: 2235, 2022.
34. Hamadouche S: Etude theorique de la reactivite des acides amines antioxydants et les aspeces reactives oxygenees: Université de batna 1, 2024.
35. Zheng J, Piao MJ, Keum YS, Kim HS and Hyun JW: Fucoxanthin protects cultured human keratinocytes against oxidative stress by blocking free radicals and inhibiting apoptosis. Biomol Ther (Seoul) 21: 270-276, 2013.
36. Heo SJ, Ko SC, Kang SM, Kang HS, Kim JP, Kim SH, Lee KW, Cho MG and Jeon YJ: Cytoprotective effect of fucoxanthin isolated from brown algae *Sargassum siliquastrum* against H_2O_2-induced cell damage. Eur Food Res Technol 228: 145-151, 2008.
37. Zhang Y, Wu H, Wen H, Fang H, Hong Z, Yi R and Liu R: Simultaneous determination of fucoxanthin and its deacetylated metabolite fucoxanthinol in rat plasma by liquid chromatography-tandem mass spectrometry. Mar Drugs 13: 6521-6536, 2015.
38. Wang S, Guo M and Jin Z: Innovative Controlled-release systems for fucoxanthin: Research progress and applications. Pharmaceutics 17: 889, 2025.
39. Koo SY, Hwang KT, Hwang S, Choi KY, Park YJ, Choi JH, Truong TQ and Kim SM: Nanoencapsulation enhances the bioavailability of fucoxanthin in microalga *Phaeodactylum tricornutum* extract. Food Chem 403: 134348, 2023.
40. Ravi H and Baskaran V: Chitosan-glycolipid nanocarriers improve the bioavailability of fucoxanthin via up-regulation of PPARγ and SRB1 and antioxidant activity in rat model. J Functional Foods 28: 215-226, 2017.
41. Ding L, Luo X, Xian Q, Zhu S and Wen W: Innovative approaches to fucoxanthin delivery: Characterization and bioavailability of solid lipid nanoparticles with Eco-Friendly ingredients and enteric coating. Int J Mol Sci 25: 12825, 2024.
42. Koo SY, Mok IK, Pan CH and Kim SM: Preparation of fucoxanthin-loaded nanoparticles composed of casein and chitosan with improved fucoxanthin bioavailability. J Agric Food Chem 64: 9428-9435, 2016.